

## Coexistence of Hydrogen Atom Transfer Reactions through and not through Triplet Ion Pair between *p*-Chloranil and Durene

Harumichi KOBASHI,\* Masa-aki FUNABASHI, Tomoyuki KONDO, Toshifumi MORITA, Tadashi OKADA,<sup>†</sup> and Noboru MATAGA<sup>†</sup>

Department of Chemistry, Faculty of Engineering, Gunma University, Kiryu, Gunma 376

<sup>†</sup>Department of Chemistry, Faculty of Engineering Science, Osaka University, Toyonaka, Osaka 560

(Received, July 13, 1984)

Mechanisms of hydrogen atom abstraction reactions by triplet state *p*-chloranil (<sup>3</sup>CA) from durene (DH) were studied by picosecond and nanosecond laser photolysis and transient photoconductivity measurements. <sup>3</sup>CA was quenched by DH through diffusional encounter to form a triplet ion pair (IP) between CA and DH, *p*-chloranil semiquinone radical (CAH<sup>•</sup>), and 2,4,5-trimethylbenzyl radical (D<sup>•</sup>). Ionic dissociation of IP was observed in 1,2-dichloroethane (DCE) as well as in acetonitrile. However, no transient species was observed by direct excitation of a charge-transfer (CT) band of the electron donor-acceptor (EDA) complex between CA and DH. The H-atom transfer leading to production of CAH<sup>•</sup> was found to proceed through two distinct mechanisms; H-atom transfer *via* IP (Mechanism I) and a more rapid transfer competing with IP formation (Mechanism II). The quantum yields of CAH<sup>•</sup> produced by Mechanisms I and II and the first-order rate constants for proton transfer, ionic dissociation, and intersystem crossing competing with one another in the IP state were estimated to be (0.1 and 0.2) and (2, 5, and 13) × 10<sup>6</sup> s<sup>-1</sup>, respectively, in DCE at room temperature.

In the case of the photochemical hydrogen abstraction reaction of triplet ketones or quinones, two different and noteworthy mechanisms have been reported. One is the two-step mechanism of electron transfer followed by proton transfer *via* ion-pair (IP) state (Mechanism I). This is the case of triplet benzophenone and several amines in high-polarity solvents<sup>1)</sup> as well as the case of the excited singlet pyrene–aromatic amines.<sup>2)</sup> Another is the rapid H-atom transfer in nonrelaxed encounter complex competing with IP formation (Mechanism II) as observed in the system of triplet state 2,6-diphenyl-*p*-benzoquinone and aromatic amines.<sup>3)</sup> Since most of the triplet state quinones are strong electron and hydrogen acceptors, it is not easy to determine which mechanism is predominant in their H abstraction reactions. Very careful examinations based on direct observation of short-lived transient species are necessary to elucidate the reaction mechanism.

In the course of our investigations concerning photo-reduction of <sup>3</sup>CA by several electron and hydrogen donors,<sup>4)</sup> we observed in the CA–DH system that CAH<sup>•</sup> radicals were produced simultaneously with the formation of IP between CA and DH and also grew up concomitantly with the decay of IP. We have examined the mechanism of this reaction mainly in DCE solution by means of picosecond (ps) and nanosecond (ns) laser photolysis and transient absorption measurements as well as transient photoconductivity studies in the ns time region. Results show coexistence of Mechanisms I and II.

### Experimental

Transient absorption spectra in the ps and ns region were measured using a mode-locked ruby laser system (λ 347 nm, FWHM ≈ 30 ps, energy ≈ 10 mJ)<sup>5)</sup> at 25 °C and a conventional ns ruby laser system<sup>6)</sup> at 20 ± 1 °C unless otherwise stated. Pho-

tolysis at 502 as well as 532 nm was also performed by using a flash-lamp pumped dye laser (dye: Green-4 of Phase-R Co., pulse width ≈ 250 ns, energy ≈ 110 mJ)<sup>6)</sup> and a ps Nd<sup>3+</sup>: YAG laser system,<sup>7)</sup> respectively. Transient photocurrents were measured using the same type of quartz cuvette with two Ni- or Pt-plate electrodes as utilized previously.<sup>8)</sup> The DC voltage (90–540 V) was supplied between the electrodes from a bank of dry batteries. The output signal across a 50 Ω load resistor was fed into a 200 MHz oscilloscope (Iwatsu, SS-6200) through AC coupling. The ground state absorption spectra were recorded on a Hitachi Model 200 spectrophotometer. All solutions were carefully degassed by freeze-pump-thaw cycles.

*p*-Chloranil (CA: tetrachloro-*p*-benzoquinone) was purified by the same method as described elsewhere.<sup>4a)</sup> The GR grade durene (DH: 1,2,4,5-tetramethylbenzene) was recrystallized twice from cyclohexane and sublimed *in vacuo*. Solvents: 1,2-dichloroethane, acetonitrile, and ethyl acetate were purified by the usual methods.

### Results and Discussion

**EDA Complex Formation in the Ground State.** The DCE solutions of CA (0.001–0.002 mol dm<sup>-3</sup>) and DH (0.075–0.40 mol dm<sup>-3</sup>) showed a CT band (λ<sub>max</sub> 480 nm; ε 2650 ± 100 dm<sup>3</sup> mol<sup>-1</sup> cm<sup>-1</sup>) due to the EDA complex (CA···DH) with the formation constant K = 0.89 ± 0.03 dm<sup>3</sup> mol<sup>-1</sup> (at 20 °C) which was determined using the Benesi-Hildebrand method. The thermodynamic quantities, ΔH (–18.1 ± 1.2 kJ mol<sup>-1</sup>) and ΔS (–63 ± 4 J mol<sup>-1</sup> K<sup>-1</sup>), were obtained by the measurement of the temperature dependence of K in the range 4–57 °C. These values are comparable with those for the same complex in carbon tetrachloride reported previously.<sup>9)</sup> The absorption spectra of the complex and uncomplexed CA involved in the DCE solution are illustrated in Fig. 1.

**Picosecond and Nanosecond Laser Photolysis.** The laser photolysis at 502 as well as 532 nm, where exclusive-

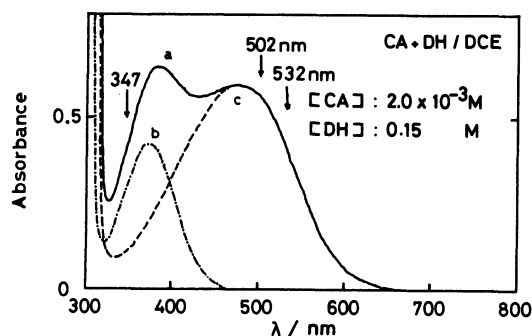


Fig. 1. Ground state absorption spectra of the CA ( $2.0 \times 10^{-3} \text{ mol dm}^{-3}$ ) and DH ( $0.15 \text{ mol dm}^{-3}$ ) system in DCE at  $18^\circ\text{C}$ . (a): observed spectrum, (b): spectrum of uncomplexed CA ( $1.76 \times 10^{-3} \text{ mol dm}^{-3}$ ) present in the solution, (c): spectrum of the EDA complex alone obtained by (a)–(b). Wavelengths of lasers used for excitation are indicated by arrows.

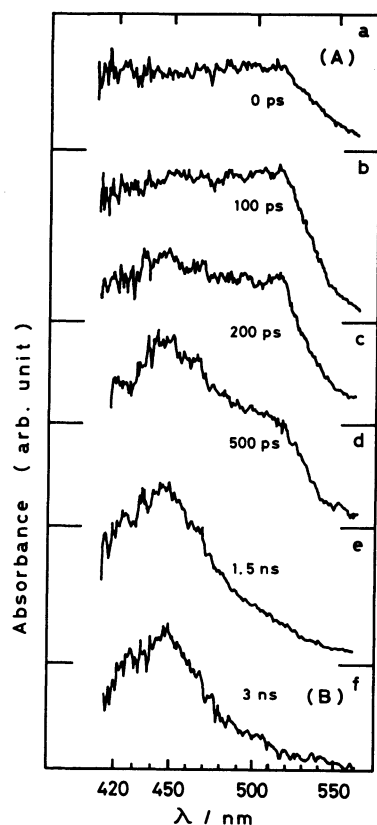


Fig. 2. Time-resolved absorption spectra obtained by the picosecond laser photolysis for the CA and DH system in DCE:

$[\text{CA}] = 3.0 \times 10^{-3} \text{ mol dm}^{-3}$ ,  $[\text{DH}] = 0.20 \text{ mol dm}^{-3}$ .

The absorbance is not corrected for shot-to-shot variations of the exciting-pulse intensity.

ly the CT band was excited (indicated by arrows in Fig. 1), did not give any transient absorption over the time range from picosecond to several microseconds. No permanent change of the ground state absorption spectrum was recognized after several laser shots. These findings suggest that the  $S_1$  state of the complex decays so rapidly through internal conversion that its detection is not possible even by means of the ps laser photo-

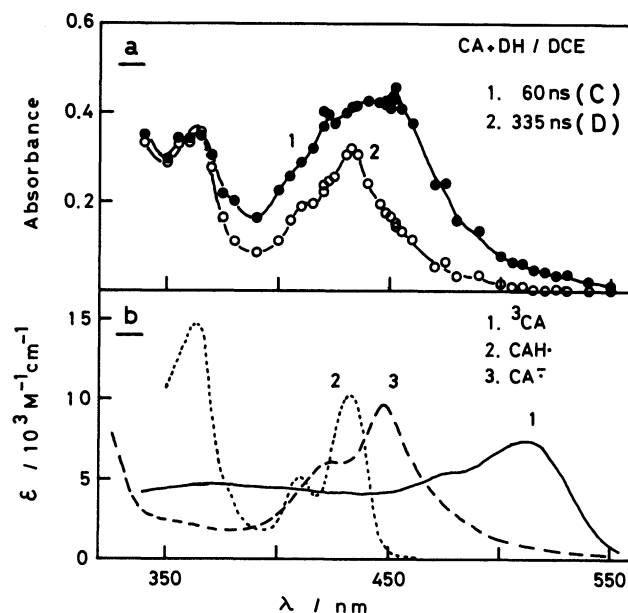


Fig. 3. a) Transient absorption spectra obtained by the nanosecond flash photolysis for the CA-DH-DCE system.

$[\text{CA}] = 3.0 \times 10^{-3} \text{ mol dm}^{-3}$ ,  $[\text{DH}] = 0.20 \text{ mol dm}^{-3}$ ; (1) 60 ns and (2) 335 ns after the beginning of laser oscillation.

b) Reference absorption spectra.

(1):  $^3\text{CA}$  in DCE, (2):  $\text{CAH}\cdot$  in DCE, (3):  $\text{CA}^-$  in acetonitrile.

lysis method. Some discussions will be given later concerning this result.

In the following we show results of the photolysis at 347 nm where excitation of uncomplexed CA is possible. Figure 2 presents time-resolved absorption spectra for the solution containing CA ( $3.0 \times 10^{-3} \text{ mol dm}^{-3}$ ) and DH ( $0.20 \text{ mol dm}^{-3}$ ) observed by the ps ruby laser photolysis. Figure 3a shows transient absorption spectra measured by the ns flash photolysis and Fig. 3b gives reference spectra of  $^3\text{CA}$ ,<sup>4a)</sup>  $\text{CAH}\cdot$ ,<sup>4b)</sup> and *p*-chloranil radical anion ( $\text{CA}^-$ ).<sup>10)</sup>

The absorption band around 510 nm in the spectrum observed at 0 ps (Fig. 2a) resembles that of  $^3\text{CA}$ . After reaching the maximum intensity, the absorbance around 510 nm decreases while a new band around 450 nm grows up. The latter absorption band is similar to that of  $\text{CA}^-$ . The spectra observed at several delay times from 100 ps to 1.5 ns could be reproduced by the superposition of the spectra at 0 ps (A) and 3 ns (B), which has been performed by a microcomputer using the least-square method. An example for the spectrum at 500 ps is given in Fig. 4, where the agreement between the calculated spectrum (b(1)) composed of A and B and the observed one (a) is satisfactory. The time dependence of each component obtained by such procedure is indicated in Fig. 5. The decay time of A and the rise time of B are estimated respectively to be about 0.7 and 0.6 ns, being in agreement with each other. This indicates that the species responsible for the spectrum B is produced from the transient which

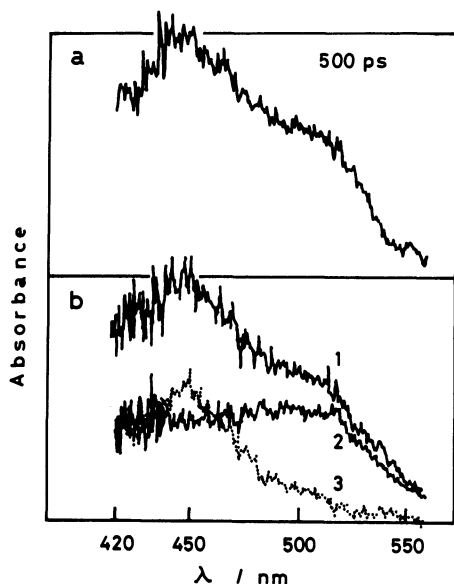


Fig. 4. Comparison of the spectrum observed at 500 ps with the spectrum obtained by superposition of A and B.

a): observed spectrum, b): (1) calculated spectrum (A+B), (2) component spectrum A, (3) component spectrum B.

shows the spectrum A.

As can be seen from Fig. 3, no absorption band around 510 nm corresponding to A was observed by the ns laser photolysis since the transient species responsible for A was quenched by DH of high concentration ( $0.20 \text{ mol dm}^{-3}$ ) very rapidly. The spectrum (C) observed immediately after excitation by the ns pulse (Fig. 3a(1)) is quite similar, in the 420–500 nm region, to the spectrum B. Therefore, it is plausible that C is substantially the same as B. Comparison of C with B in the wavelength region less than 420 nm was not possible because of the absence of observed band in the case of B owing to the low intensity of the ps probe pulse.

The spectrum C is replaced completely by the spectrum (D) with definite absorption maxima at 435 and 365 nm and a shoulder around 448 nm at the delay time of 335 ns. The decay profile of the absorbance at 448 nm is shown in Fig. 6, which indicates the existence of two components. Since the long-lived component did not show decay in 100 ns domain, we subtracted its absorbance ( $D_\infty$ ) from the observed total absorbance  $D$ . A straight line (b) obtained by plotting  $\log(D - D_\infty)$  against time yields the decay time ( $\tau_d$ ) of  $49 \pm 2 \text{ ns}$  at  $20^\circ\text{C}$  of the transient species responsible for the band at 448 nm. The  $\tau_d$  values were independent on [CA] in the  $(0.81\text{--}3.65) \times 10^{-3} \text{ mol dm}^{-3}$  range, [DH] in the  $0.05\text{--}0.20 \text{ mol dm}^{-3}$  range, and on monitoring wavelength in the 448–480 nm region, within experimental accuracy.

**Assignment of Transient Spectra and Reaction Mechanism.** Since no transient absorption was observed by direct excitation of the EDA complex, only free CA present

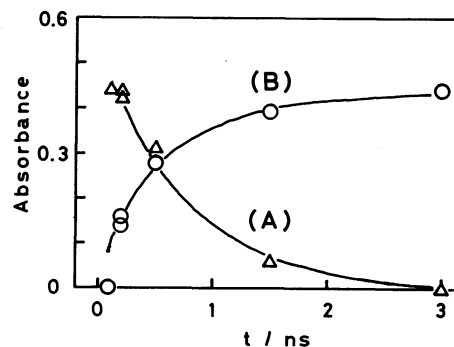


Fig. 5. Time dependence of absorbances of spectrum A at 510 nm ( $\Delta$ ) and spectrum B at 448 nm ( $\circ$ ). Absorbances are corrected for variations of the laser intensity.

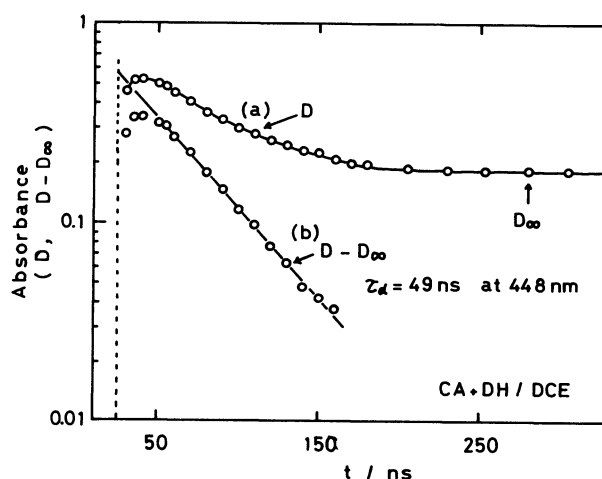


Fig. 6. Semi-logarithmic plots of absorbance at 448 nm vs. time in the CA–DH–DCE system. (a):  $\log D$  vs.  $t$ , (b):  $\log(D - D_\infty)$  vs.  $t$ .

in the solution seems to contribute to the appearance of A. Excited CA is known to cause rapid intersystem crossing (ISC,  $k_{\text{ISC}} \approx 3 \times 10^{10} \text{ s}^{-1}$ ,  $\Phi_{\text{ISC}} = 1$ ) from  $S_1$  to  $T_1$  in acetonitrile.<sup>11</sup> We have also confirmed that ISC is also rapid ( $> 3 \times 10^{10} \text{ s}^{-1}$ ) in the DCE solution of CA ( $0.003 \text{ mol dm}^{-3}$ )–diphenylamine ( $0.1 \text{ mol dm}^{-3}$ ) system in a separate experiment performed by means of the  $\text{Nd}^{3+}$ : YAG laser photolysis.<sup>12</sup> Therefore, the spectrum A can be assigned to that of  $^3\text{CA}$ .<sup>13</sup>

As shown in Fig. 3b,  $\text{CA}^-$  shows a strong band with maximum at 448 nm where  $\text{CAH}^\cdot$  shows only a negligibly weak absorption. Therefore, the absorption band at 448 nm in B, C, and D can be attributed to  $\text{CA}^-$ . Figure 5 shows that  $\text{CA}^-$  in question is produced in the course of the collisional quenching of  $^3\text{CA}$  by DH, since  $^3\text{CA}$  is quenched by DH with nearly diffusion-controlled rate.<sup>14</sup> However, the transient species showing the 448 nm absorption in C (*i.e.*, B) is not free  $\text{CA}^-$  because its decay obeys the first-order kinetics (Fig. 6b). Accordingly, this absorption band at 448 nm can be assigned to  $\text{CA}^-$  of the triplet ion pair  $^3(\text{CA}^- \cdots \text{DH}^+)$ . The spin state should be assigned to the triplet state because the observed species with a fairly long life was produced from the triplet state precursor while no

CT singlet state  $^1(\text{CA}^{\cdot-} \cdots \text{DH}^+)$ , which should be produced by the direct excitation of the CT band, was observed. That no absorption band due to the counter ion  $\text{DH}^+$  was detected is probably due to its low intensity in the visible region.<sup>15)</sup> The ion-pair formation may be rationalized also from the following estimations concerning the free energy change  $\Delta G$  of the reaction  $^3\text{CA} + \text{DH} \rightarrow ^3(\text{CA}_s^{\cdot-} \cdots \text{DH}_s^+)$  or  $^3(\text{CA}^{\cdot-} \cdots \text{DH}^+)_s$ , where  $^3(\text{CA}_s^{\cdot-} \cdots \text{DH}_s^+)$  represents the solvent-separated ion pair and  $^3(\text{CA}^{\cdot-} \cdots \text{DH}^+)_s$  refers to the contact ion pair or the triplet exciplex with nearly complete CT character. The quenching of  $^3\text{CA}$  is not attributable to the T-T energy transfer,  $^3\text{CA} + \text{DH} \rightarrow \text{CA} + ^3\text{DH}$ , in view of the fact that the energy of  $^3\text{CA}$  above the ground state ( $E_T(^3\text{CA}) \approx 2.13 \text{ eV}$ <sup>16)</sup>) is much lower than that of  $^3\text{DH}$  ( $E_T(^3\text{DH}) = 3.37 \text{ eV}$ ).<sup>17)</sup> The  $\Delta G$  values of the ion-pair formation in DCE are estimated approximately to be  $-0.43 \text{ eV}$  for  $^3(\text{CA}_s^{\cdot-} \cdots \text{DH}_s^+)$  by the equation:<sup>18)</sup>

$$\begin{aligned} \Delta G(\text{CA}_s^{\cdot-} \cdots \text{DH}_s^+) &= E(\text{DH}/\text{DH}^+) - E(\text{CA}^{\cdot-}/\text{CA}) \\ &\quad - E_T(^3\text{CA}) - e^2/\epsilon R + (e^2/2)(1/R_+ + 1/R_-)(1/\epsilon - 1/37.5), \end{aligned} \quad (1)$$

and  $-0.73 \text{ eV}$  for  $^3(\text{CA}^{\cdot-} \cdots \text{DH}^+)_s$  by<sup>19)</sup>

$$\begin{aligned} \Delta G(\text{CA}^{\cdot-} \cdots \text{DH}^+)_s &= E(\text{DH}/\text{DH}^+) - E(\text{CA}^{\cdot-}/\text{CA}) \\ &\quad - E_T(^3\text{CA}) + 0.32 - 0.7[f(\epsilon) - 0.5f(n^2)] \end{aligned} \quad (2)$$

in eV unit, where  $E(\text{DH}/\text{DH}^+)$  and  $E(\text{CA}^{\cdot-}/\text{CA})$  are the polarographic oxidation potential of DH (1.59 V)<sup>20)</sup> and the reduction potential of CA (0.01 V)<sup>21)</sup> respectively,  $\epsilon$  and  $n$  are the dielectric constant and refractive index of solvent respectively,  $f(x) = 2(x-1)/(2x+1)$ , and other symbols and parameter values are the same as used in the references. Since both values of  $\Delta G$  are negatively

large, the electron transfer would occur to form the ion pairs. Contact and solvent-separated ion pairs have been discriminated in some EDA systems.<sup>1c,3b,22,23)</sup> However, the discrimination between them was not possible for the present system in DCE solution. Therefore, we use throughout this paper the term "triplet ion pair (IP)," without discrimination between contact and solvent-separated ion pairs, for the species exhibiting the 448 nm band in the spectrum C (and B) with the lifetime of 49 ns.

The spectra C and D in Fig. 3a appear at first glance to resemble the reference spectra of  $\text{CA}^{\cdot-}$  and  $\text{CAH}^{\cdot}$  respectively but close inspection makes clear the differences between them. The ratio of 435 to 448 nm absorbance in C is significantly higher than the corresponding ratio in the reference spectrum of  $\text{CA}^{\cdot-}$  and additionally C involves the band at 365 nm which is characteristic of  $\text{CAH}^{\cdot}$ . In the spectrum D, the intensity ratio of 365 to 435 nm band is small compared with that of  $\text{CAH}^{\cdot}$  and the shoulder around 448 nm which is characteristic of  $\text{CA}^{\cdot-}$  is observed. It is, therefore, suggested that both spectra C and D involve the absorption bands of the two species  $\text{CAH}^{\cdot}$  and  $\text{CA}^{\cdot-}$ . The decomposition of the spectrum into  $\text{CAH}^{\cdot}$  and  $\text{CA}^{\cdot-}$  was then performed very carefully and the result is given in Fig. 7. The procedure for decomposition was made by normalizing the reference spectrum of  $\text{CA}^{\cdot-}$  to the observed one at 448 nm and then subtracting the former from the latter. The obtained spectrum (Fig. 7a (3)) agrees with the spectrum of  $\text{CAH}^{\cdot}$ . A small difference between the spectrum of  $\text{CA}^{\cdot-}$  and the observed one (C) in the wavelength region longer than 448 nm seems attributable to a small difference in the spectra between IP and free  $\text{CA}^{\cdot-}$ . The spectrum D can be reproduced quite well by superposing spectra of  $\text{CAH}^{\cdot}$  and  $\text{CA}^{\cdot-}$  (Fig. 7b). Since, as is shown in Fig. 8, the 448 nm absorbance in D shows the second order decay, this absorption band may be assigned to free  $\text{CA}^{\cdot-}$ . From the results of the analysis indicated in Fig. 7, it can be concluded that  $\text{CAH}^{\cdot}$  radicals are rapidly produced in part competitively with IP formation and further increase in accordance with decrease of IP.

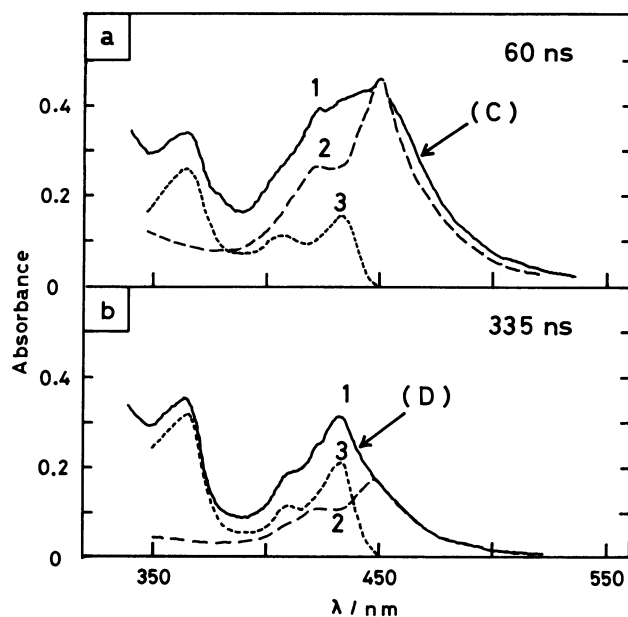


Fig. 7. Spectrum decomposition for the spectra in Fig. 3a observed at 60 ns (a) and at 335 ns (b); (1) observed spectrum, (2) spectrum of  $\text{CAH}^{\cdot}$  component (3) (1)–(2).

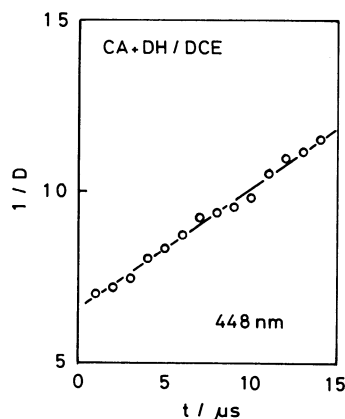


Fig. 8. A second-order decay plot for the spectrum D at 448 nm.

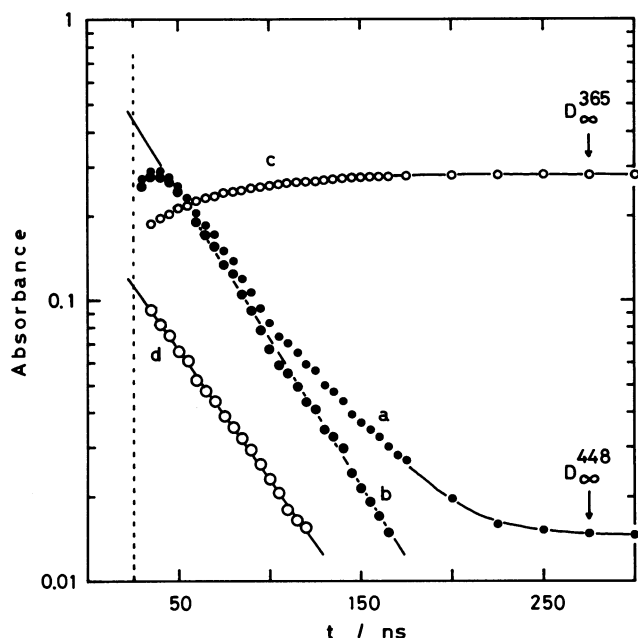


Fig. 9. Time dependence of 365 and 448 nm absorbances observed in ethyl acetate solution of CA ( $0.0011 \text{ mol dm}^{-3}$ ) and DH ( $0.20 \text{ mol dm}^{-3}$ ): (a)  $\log D$  vs.  $t$  and (b)  $\log (D - D_{\infty})$  vs.  $t$  measured at 448 nm, (c)  $\log D$  vs.  $t$  and (d)  $\log (D_{\infty} - D)$  vs.  $t$  measured at 365 nm.

Therefore, it is confirmed that the H-atom transfer in problem proceeds through both Mechanisms I and II.

Although in DCE solution the slow rise of CAH $\cdot$  was established on the basis of the result of spectrum decomposition, the rise was observed directly by monitoring the characteristic absorption band of CAH $\cdot$  at 365 or 435 nm in other less polar solvents. Figure 9 shows time dependence of 365 nm absorbance,  $D_{365}^{365}$ , (line c) together with that of 448 nm absorbance,  $D_{448}^{448}$ , (line a) observed in ethyl acetate solution. The line b is the plot of  $D_{448}^{448} - D_{\infty}^{448}$  against  $t$  yielding the decay time ( $\tau_d$ ) of IP. The line d is the plot of  $D_{365}^{365} - D_{\infty}^{365}$ , yielding the rise time ( $\tau_r$ ) of CAH $\cdot$ . Here,  $D_{448}^{448}$  and  $D_{365}^{365}$  are the absorbances in the plateau region observed at 448 and 365 nm, respectively. It is clear that CAH $\cdot$  grows up concomitantly with decay of IP because  $\tau_r$  value (51 ns) agrees with  $\tau_d$  value (47 ns) within experimental accuracy.

The formation of free ions as noted in the discussion of the spectrum **D** was examined by transient photoconductivity measurement. Figure 10 demonstrates the oscillograms of photocurrent together with the temporal behavior of transient absorption. The rise time ( $50 \pm 3 \text{ ns}$  from 5 runs) of the photocurrent was in good agreement with the decay time of IP and the decay of the current followed exactly the second-order kinetics. It is therefore confirmed that the ionic dissociation producing free CA $^{\cdot-}$  occurs subsequent to the IP formation.

In addition to these measurements, we have observed a fairly sharp absorption band around 330 nm

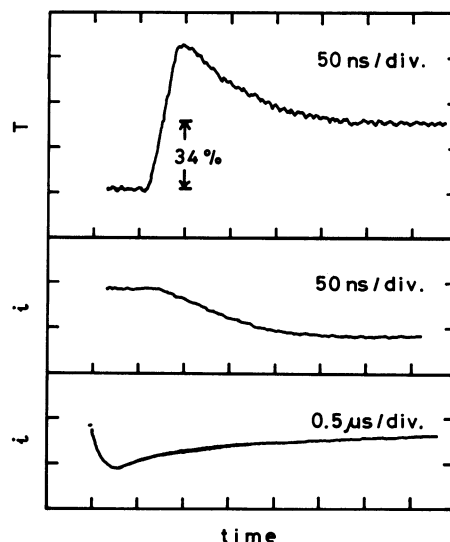
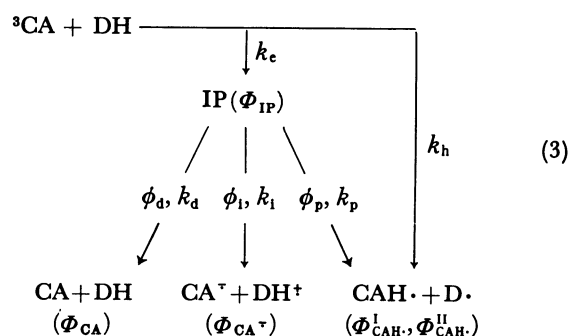


Fig. 10. Oscilloscope traces for transient absorption (T: transmittance) monitored at 448 nm (a) and transient photocurrents ( $i \approx 0.1 \text{ mA/div}$ ), (b) and (c), in DCE solution:

[CA] =  $0.0025 \text{ mol dm}^{-3}$ , [DH] =  $0.20 \text{ mol dm}^{-3}$ .

simultaneously with the bands of CAH $\cdot$ . This observation suggests strongly the pair production of CAH $\cdot$  and 2,4,5-trimethylbenzyl radical (D $\cdot$ ), because D $\cdot$  has a sharp band at 330 nm.<sup>24)</sup>

From the above described results, the deactivation processes of  $^3\text{CA}$  by the interaction with DH may be schematically represented as follows:



Here, the letters  $\Phi$ ,  $\phi$ , and  $k$  represent the quantum yield of transient species from  $^3\text{CA}$ , the fractional efficiency of each reaction from IP, and the rate constant of each reaction process, respectively. The subscripts e, h, p, i, and d refer in turn to the processes of electron transfer, hydrogen transfer, proton transfer, ionic dissociation, and degradation through ISC of IP returning back to the ground state.  $\Phi_{\text{CAH}\cdot}^{\text{I}}$  and  $\Phi_{\text{CAH}\cdot}^{\text{II}}$  denote the quantum yields of CAH $\cdot$  formation by the mechanism I and II, respectively. Estimation for these values measured in DCE solution will be given in the later section.

*No Transient Formation by Direct Excitation of the EDA Complex.* We examine here the mechanism

for the result that direct photoexcitation into the CT band of the complex affords no transient absorption. The energy levels of locally excited (LE) singlet  $^1(\text{CA}^* \dots$

DH) and triplet  $^3(\text{CA}^*\cdots\text{DH})$  states may be approximately the same as those of  $^1\text{CA}^*+\text{DH}$  and  $^3\text{CA}^*+\text{DH}$  states which lie in 2.63<sup>25)</sup> and 2.31 eV<sup>16)</sup> above the  $\text{CA}+\text{DH}$  state, respectively. The energies of CT singlet  $^1(\text{CA}^-\cdots\text{DH}^+)$  and triplet  $^3(\text{CA}^-\cdots\text{DH}^+)$  states may be given approximately as 1.7 and 1.3 eV, respectively, from the position of onset of the CT band and from the energy of  $^3(\text{CA}^-\cdots\text{D}^+)$  state estimated by using Eq. 2. Since the energy gap between zero-order  $^1\text{CT}$  and  $^1\text{LE}$  states is large, their mixing will be small. This condition results in small splitting between  $^1\text{CT}$  and  $^3\text{CT}$  states. In practice,  $^1(\text{CA}^-\cdots\text{DH}^+)$  and  $^3(\text{CA}^-\cdots\text{DH}^+)$  states will lie closer to each other than the expectation from the above estimation owing to the intra-complex as well as stabilization induced by solvent reorientation in  $^1(\text{CA}^-\cdots\text{DH}^+)$ . In any way, these  $^1(\text{CA}^-\cdots\text{DH}^+)$  and  $^3(\text{CA}^-\cdots\text{DH}^+)$  states will be the lowest excited singlet and triplet states, respectively, and  $^3(\text{CA}^*\cdots\text{DH})$  state will locate higher than  $^1(\text{CA}^-\cdots\text{DH}^+)$  state.

The fact that no transient formation was observed in the case of direct excitation of EDA complex means that ISC does not take place effectively in the complex from the  $^1\text{CT}$  state to the  $^3\text{CT}$  state. This is also supported by the fact that no CT phosphorescence could be observed at low temperature. ISC between the CT states is forbidden since the matrix element of spin-orbit interaction,  $\langle ^1\text{CT} | \hat{H}_{\text{SO}} | ^3\text{CT} \rangle$  which governs the ISC rate, becomes null in the usual one-electron approximation. Therefore, ISC may be unfavorable to take place competing with the allowed internal conversion from the  $^1\text{CT}$  state to the ground state. Since no LE state lies between the  $^1\text{CT}$  and  $^3\text{CT}$  states, the conclusion inferred above is in harmony with the selection rule proposed by Lim *et al.* for the systems of tetracyanoethylene-methylated benzenes and 1,2,4,5-tetracyanobenzene-methylated benzenes.<sup>26)</sup> The internal conversion would be so rapid that no transient species was observed even by the present ps time resolution. Similar results of ps laser photolysis studies have been reported also for the duroquinone-triethylamine,<sup>27a)</sup> porphyrin-quinone,<sup>27b)</sup> and pyrene-pyromellitic dianhydride<sup>27c)</sup> systems.

*Yields of IP, CAH·, and CA<sup>-</sup> and Rate Constants for Decay Processes of IP.* Estimation of  $\Phi_{\text{IP}}$ ,  $\Phi_{\text{CAH}}^{\text{II}}$ ,  $k_e$ , and  $k_h$ : Since the triplet yield of CA has been known to be unity,<sup>4a, 11b)</sup>  $\Phi_{\text{IP}}$  can be estimated from Fig. 5 using Eq. 4:

$$\Phi_{\text{IP}} = \frac{D_{\text{IP}}(3)/\epsilon_{\text{IP}}}{D_{3\text{CA}}(0)/\epsilon_{3\text{CA}}}, \quad (4)$$

where  $D_{\text{IP}}(3)$  is the 448 nm absorbance due to IP at 3 ns,  $D_{3\text{CA}}(0)$  is the 510 nm absorbance of  $^3\text{CA}$  at 0 ps,  $\epsilon_{\text{IP}}$  is the molar absorption coefficient of IP at 448 nm ( $9.0 \times 10^3 \text{ dm}^3 \text{ mol}^{-1} \text{ cm}^{-1}$ )<sup>28)</sup> and  $\epsilon_{3\text{CA}}$  is that of  $^3\text{CA}$  in DCE at 510 nm,  $(7.3 \pm 0.3) \times 10^3 \text{ dm}^3 \text{ mol}^{-1} \text{ cm}^{-1}$ .<sup>29)</sup> The  $\Phi_{\text{IP}}$  value obtained is 0.81 within the error of about 10%.  $\Phi_{\text{CAH}}^{\text{II}}$  value is obtained to be 0.19 by the relation  $\Phi_{\text{CAH}}^{\text{II}} = 1 - \Phi_{\text{IP}}$  according to (3). By using the

quenching rate constant of  $^3\text{CA}$  by DH measured at 15°C,<sup>14)</sup> approximate values of second-order rate constants,  $k_e$  and  $k_h$ , are estimated to be  $2.5 \times 10^9 \text{ dm}^3 \text{ mol}^{-1} \text{ s}^{-1}$  and  $0.6 \times 10^9 \text{ dm}^3 \text{ mol}^{-1} \text{ s}^{-1}$ , respectively.

*Determination of  $\Phi_{\text{CAH}}^{\text{total}}$ ,  $\Phi_{\text{CA}^-}$ ,  $\Phi_{\text{CAH}}^{\text{I}}$  and  $\Phi_{\text{CA}}$ :* For the purpose of obtaining the total yields of  $\text{CAH} \cdot$  ( $\Phi_{\text{CAH}}^{\text{total}} \equiv \Phi_{\text{CAH}}^{\text{I}} + \Phi_{\text{CAH}}^{\text{II}}$ ) and  $\Phi_{\text{CA}^-}$  values, the ns laser photolysis was carried out, under the same laser intensity, for solutions of CA in the presence and absence of DH. The absorbances at 347 nm of the solutions were adjusted equal to each other. The solutions containing CA alone were used as references for the yield of  $^3\text{CA}$ . Then,  $\Phi_{\text{CAH}}^{\text{total}}$  and  $\Phi_{\text{CA}^-}$  can be expressed by Eqs. 5 and 6 respectively using transient absorbances measured at 300 ns after the laser excitation.

$$\Phi_{\text{CAH}}^{\text{total}} = \frac{D_{\text{CAH}}/\epsilon_{\text{CAH}}}{D_{3\text{CA}}^{\text{calc}}/\epsilon_{3\text{CA}}}, \quad (5)$$

$$\Phi_{\text{CA}^-} = \frac{D_{\text{CA}^-}/\epsilon_{\text{CA}^-}}{D_{3\text{CA}}^{\text{calc}}/\epsilon_{3\text{CA}}}, \quad (6)$$

where  $D_{\text{CAH}}$  and  $D_{\text{CA}^-}$  are the absorbances of  $\text{CAH} \cdot$  at 435 nm and  $\text{CA}^-$  at 448 nm after the spectrum decomposition, respectively, and  $D_{3\text{CA}}^{\text{calc}} \equiv D_{3\text{CA}} \cdot D_{\text{CA}}^0 / (D_{\text{CA}}^0 + D_{\text{DH}}^0)$  is the calculated absorbance of  $^3\text{CA}$  which should be produced in the mixed solution of CA and DH immediately after the excitation.  $D_{3\text{CA}}$  is the 510 nm absorbance of  $^3\text{CA}$  observed in the reference solution of CA.  $D_{\text{CA}}^0$  and  $D_{\text{DH}}^0$  are the 347 nm absorbances of uncomplexed CA and complex  $\text{CA} \cdots \text{DH}$  respectively and hence  $D_{\text{CA}}^0 / (D_{\text{CA}}^0 + D_{\text{DH}}^0)$  means the fraction of absorbance due to free CA present in the mixed solution to the total absorbance at 347 nm.  $\epsilon_{\text{CAH}}$  is the molar absorption coefficient of  $\text{CAH} \cdot$  in DCE ( $1.0 \times 10^4 \text{ dm}^3 \text{ mol}^{-1} \text{ cm}^{-1}$  at 435 nm)<sup>30)</sup> and  $\epsilon_{\text{CA}^-}$  is that of  $\text{CA}^-$  ( $9.0 \times 10^3 \text{ dm}^3 \text{ mol}^{-1} \text{ cm}^{-1}$  at 448 nm).<sup>28b, 31)</sup> Table I shows results obtained. Although rather large error (about 20%) was presumed for each  $\Phi$  value, the agreement among several measurements for each pair of solutions was good (within 10%). Both values of  $\Phi_{\text{CAH}}^{\text{total}}$  and  $\Phi_{\text{CA}^-}$  are independent on  $[\text{CA}]$  as well as  $[\text{DH}]$ .  $\Phi_{\text{CAH}}^{\text{I}}$  was evaluated to be 0.10 by using the relation  $\Phi_{\text{CAH}}^{\text{I}} = \Phi_{\text{CAH}}^{\text{total}} - \Phi_{\text{CAH}}^{\text{II}}$  with the value of  $\Phi_{\text{CAH}}^{\text{II}} = 0.19$ . The  $\Phi_{\text{CA}}$  value was calculated to be 0.52 by  $\Phi_{\text{CA}} = 1 - \Phi_{\text{CAH}}^{\text{total}} - \Phi_{\text{CA}^-}$ . If the quenching of  $^3\text{CA}$  yielding no transient species is competing with IP formation in

TABLE I. YIELDS OF  $\text{CAH} \cdot$  AND  $\text{CA}^-$  IN DCE AT 20°C

[CA] / $10^{-3} \text{ mol dm}^{-3}$	[DH] / $10^{-1} \text{ mol dm}^{-3}$	$\Phi_{\text{CAH}}^{\text{total}}$	$\Phi_{\text{CA}^-}$
2.0	0.1	0.29	0.18
2.0	1.0	0.29	0.17
2.0	1.5	0.28	0.19
2.0	2.0	0.28	0.21
2.0	2.5	0.29	0.21
2.5	1.0	0.29	0.20
2.0	1.0	0.30	0.19
1.5	1.0	0.28	0.19
av.		0.29	0.19

the encounter complex,  $\Phi_{CA}$  must satisfy the relation  $\Phi_{CA}=1-\Phi_{IP}-\Phi_{CAH}^H<1-\Phi_{IP}=0.19$ . This relation contradicts the experimental result ( $\Phi_{CA}=0.52$ ), so that the deactivation to the ground state competing with IP formation may be neglected in (3).

**Determination of  $\phi_p$ ,  $\phi_i$ ,  $\phi_d$ ,  $k_p$ ,  $k_i$ , and  $k_d$ :** Using the  $\Phi$  values together with the  $\tau_d$  value the efficiencies ( $\phi$ ) for decay channels of IP and the first-order rate constants ( $k$ ) for the corresponding processes could be estimated as follows:

$$\begin{aligned}\phi_p &= 0.12, & k_p &= 2 \times 10^6 \text{ s}^{-1}, \\ \phi_i &= 0.23, & k_i &= 5 \times 10^6 \text{ s}^{-1}, \\ \phi_d &= 0.65, & k_d &= 13 \times 10^6 \text{ s}^{-1}.\end{aligned}\quad (7)$$

On the other hand, from the time dependence of absorbances obtained by the ns laser photolysis alone, we could also estimate  $\phi_p=0.14$  by Eq. 8,

$$\phi_p = \frac{\{D_{CAH\cdot}(300) - D_{CAH\cdot}(50)\}/\epsilon_{CAH\cdot}}{D_{448}(50)/\epsilon_{IP}} \quad (8)$$

assuming that  $D_{448}(50)$ , the 448nm absorbance observed at 50ns, is due to IP. In Eq. 8,  $D_{CAH\cdot}(50)$  and  $D_{CAH\cdot}(300)$  are the absorbances of  $CAH\cdot$  at 435nm (after the spectrum decomposition) measured at 50 and 300ns, respectively, and  $\epsilon_{CAH\cdot}$  and  $\epsilon_{IP}$  are the same as in Eqs. 5 and 6.

For the purpose of comparison we present here briefly some results obtained in the CA-diphenylamine (DPA)-DCE system.<sup>12</sup> We have found the triplet IP,  $^3(CA^-\cdots DPA^+)$ , with a lifetime of *ca.* 8ns,  $k_i \approx 1 \times 10^7 \text{ s}^{-1}$ , and  $k_d \approx 1.1 \times 10^8 \text{ s}^{-1}$ , whereas no proton transfer in  $^3(CA^-\cdots DPA^+)$  has been detected. The  $k_p$  value given in Eq. 7 is much less than the corresponding values for benzophenone (BP)-*N,N*-dimethylaniline (DMA) system ( $k_p=2.0 \times 10^9 \text{ s}^{-1}$  in acetonitrile)<sup>13</sup> and pyrene (P)-primary or secondary aromatic amine system (*e.g.*, ( $k_p=5 \times 10^9 \text{ s}^{-1}$  for P-DPA system in toluene).<sup>2</sup> Although the number of data of  $k_p$  value in Mechanism I is still scarce for any detailed discussion, these data appear to indicate that the rate of proton transfer in IP decreases with increase of the free energy change of this reaction.<sup>32</sup> In Eq. 7, the  $k_i$  value is larger than the  $k_p$  value by a factor of about 2.5. However, the rate of ionic dissociation in DCE is much slower than that in acetonitrile, where the photocurrent has been found to reach its maximum intensity immediately after the pulsing (Fig. 11). Therefore, the slow dissociation in DCE

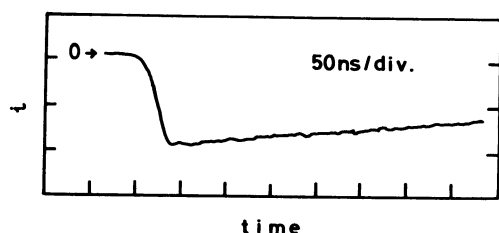


Fig. 11. Transient photocurrent measured in acetonitrile.

may be largely dependent on a fairly strong binding by Coulomb force between the ions in IP, which does not contradict the fact that both  $k_i$  values for  $^3(CA^-\cdots DH^+)$  and  $^3(CA^-\cdots DPA^+)$  are close to each other. It is known that the ionic dissociation to free ions occurs from solvent-separated ion pair (SSIP)<sup>22</sup> while the proton transfer takes place from contact ion pair (CIP).<sup>13</sup> From the fact that the rise time of photocurrent is equal to the decay time of IP, it may be inferred that IP observed here in DCE comprises both CIP and SSIP in equilibrium with each other. It is often used that because of spin-forbidden nature a back electron-transfer in triplet IP leading to the ground state cannot compete with ionic dissociation. However, in DCE of moderately polar solvent the back electron-transfer ( $k_d$ ) can take place effectively rather than the ionic dissociation ( $k_i$ ). Similar observation about the competition between  $k_d$  and  $k_i$  processes has been reported for various quinone-aromatic amine systems.<sup>33</sup> Moreover, the  $k_d$  value ( $\approx 1.1 \times 10^8 \text{ s}^{-1}$ ) for  $^3(CA^-\cdots DPA^+)$  obtained by us in DCE agrees well with  $k_d=1.1 \times 10^8 \text{ s}^{-1}$  obtained by a different procedure in benzene-benzonitrile mixture.<sup>30</sup> The  $k_d$  value in  $^3(CA^-\cdots DH^+)$  is of one order of magnitude smaller than that in  $^3(CA^-\cdots DPA^+)$ . This tendency is parallel to the linear relation between  $\log k_d$  and the energy level of IP above the ground state,<sup>33</sup> since the energy of  $^3(CA^-\cdots DPA^+)$  is estimated by Eq. 2 to be lower by 0.81 eV than that of  $^3(CA^-\cdots DH^+)$ . Hence, it seems to indicate that ISC of IP obeys the energy gap law of radiationless transition.

**Competition of Mechanisms I and II.** Finally we consider the mechanism of competition of I and II. A key point determining the mechanism must be involved in a collision complex between  $^3CA$  and  $DH$ . Since in the present case  $DH$  approaches by diffusion to  $^3CA$  from random directions, the collision complex with various donor-acceptor configurations might be produced. It may be true that an electron transfer occurs depending principally on the separation distance but not so severely on the mutual orientation between donor and acceptor. On the other hand, H-atom transfer will depend strongly on the local disposition of the transfer sites in the collision complex. Therefore, difference in conformations of the collision complexes seems to reflect the difference in the mechanisms of H-atom transfer. In the present case, it is supposed that a large part (about 80%) of the collision complexes can take conformations favorable to cause the electron transfer followed by immediate relaxation to the IP state; *e.g.*, a conformation with face to face approach between the donor and the acceptor. The other collision complexes of about 20% would take some special conformations favorable to undergo the rapid H-atom transfer; *e.g.*, a conformation with the transfer sites very close to each other like a hydrogen bonding bridge between O-atom of the acceptor and H-atom of methyl groups on the donor. Such a rapid H-atom transfer in the collision complex has been suggested for the dynamic quench-

ing in the hydrogen bonding interaction systems such as 2-naphthol-pyridine-cyclohexane system<sup>34</sup> as well as the quenching of triplet quinones by aromatic amines.<sup>3</sup> Recently, very fast H-atom transfer by a two-step mechanism of electron transfer followed by proton transfer has been verified both in EDA systems<sup>1,2</sup> and in hydrogen bonding interaction systems.<sup>18,35</sup> Taking these facts into account, it seems that the rapid H-atom transfer observed here also proceeds through the mechanism by transitory electron transfer preceding proton transfer.<sup>36</sup> Therefore, it may be interpreted that the first event of the quenching is an electron transfer from DH to <sup>3</sup>CA and successively, in the collision complex, a rapid proton transfer and relaxation to the IP state compete with each other. The net H-atom transfer by Mechanism I occurs relatively slowly depending on the rate of proton transfer in IP. This suggests that a fairly high potential barrier is necessary to take a conformation favorable for causing the proton transfer from the relaxed state IP. A detailed study of the temperature dependence of this process will be published in a separate paper.

## References

- 1) a) K. S. Peters, S. C. Freilich, and C. G. Schaeffer, *J. Am. Chem. Soc.*, **102**, 5701 (1980); b) C. C. Shaefer and K. S. Peters, *J. Am. Chem. Soc.*, **102**, 7566 (1980); c) J. D. Simon and K. S. Peters, *J. Am. Chem. Soc.*, **103**, 6403 (1981).
- 2) a) T. Okada, N. Tashita, and N. Mataga, *Chem. Phys. Lett.*, **75**, 220 (1980); b) T. Okada, I. Karaki, and N. Mataga, *J. Am. Chem. Soc.*, **104**, 7191 (1982).
- 3) a) V. A. Kuzmin, A. P. Darmanyan, and P. P. Levin, *Chem. Phys. Lett.*, **63**, 509 (1979); b) P. P. Levin, A. P. Darmanyan, V. A. Kuzmin, A. Z. Yankelovich, and V. M. Kuznets, *Bull. Acad. Sci. USSR, Div. Chem. Sci.*, **29**, 1919 (1980); c) P. P. Levin and T. A. Kokrashvili, *Bull. Acad. Sci. USSR, Div. Chem. Sci.*, **30**, 971 (1981).
- 4) a) H. Kobashi, H. Gyoda, and T. Morita, *Bull. Chem. Soc. Jpn.*, **50**, 1731 (1977); b) H. Kobashi, T. Nagumo, and T. Morita, *Chem. Phys. Lett.*, **57**, 369 (1978); c) H. Kobashi, Y. Tomioka, and T. Morita, *Bull. Chem. Soc. Jpn.*, **52**, 1568 (1979); d) H. Kobashi, E. Sunoh, and T. Morita, *Symposium on Photochemistry*, Tokyo, December 1979, Abstr. No. BIII-210; *Chem. Abstr.*, **93**, 45538t (1980).
- 5) T. Okada, M. Migita, N. Mataga, Y. Sakata, and S. Misumi, *J. Am. Chem. Soc.*, **103**, 4715 (1981).
- 6) H. Shioyama, H. Masuhara, and N. Mataga, *Chem. Phys. Lett.*, **88**, 161 (1982).
- 7) H. Masuhara, N. Ikeda, M. Miyasaka, and N. Mataga, *J. Spectrosc. Soc. Jpn.*, **31**, 19 (1982).
- 8) Y. Taniguchi, Y. Nishina, and Mataga, *Bull. Chem. Soc. Jpn.*, **45**, 764 (1972).
- 9) G. Briegleb, "Elektron-Donor-Acceptor-Komplexe," Springer-Verlag, Berlin (1962).
- 10) J. J. Andre and G. Weil, *Mol. Phys.*, **15**, 97 (1968).
- 11) a) E. F. Hilinski, S. V. Milton, and P. M. Rentzepis, *J. Am. Chem. Soc.*, **105**, 5193 (1983); b) R. Gschwind and E. Haselbach, *Helv. Chim. Acta*, **62**, 941 (1979).
- 12) Details will be published elsewhere.
- 13) The spectrum A appears slightly diffuse compared with the reference spectrum of <sup>3</sup>CA. Although there may be a possibility that the diffuseness is due to contribution of a broad Sn—S<sub>1</sub> absorption of CA,<sup>11</sup> its contribution seems here to be minor even if present.
- 14) The quenching rate constant  $k_q$  was measured by us to be  $3.1 \times 10^9 \text{ dm}^3 \text{ mol}^{-1} \text{ s}^{-1}$  at 15°C in the low concentration range (0.001–0.0075 mol dm<sup>-3</sup>) of the quencher DH.
- 15) K. Schested, J. Holcman, and E. J. Hart, *J. Phys. Chem.*, **81**, 1363 (1977).
- 16) N. A. Shcheglova, D. N. Shigoline, G. G. Yakobson, and L. Sh. Tushishvili, *Zh. Fiz. Khim.*, **43**, 1984 (1969).
- 17) H. Spöner and Y. Kanda, *J. Chem. Phys.*, **40**, 778 (1964).
- 18) a) N. Ikeda, T. Okada, and N. Mataga, *Bull. Chem. Soc. Jpn.*, **54**, 1025 (1981); b) A. Weller and K. Zachariasse, "Molecular Luminescence," ed by E. C. Lim, Benjamin, New York (1969) p. 895.
- 19) a) H. Beens and A. Weller, "Organic Molecular Photophysics," Vol. 2, ed. by J. B. Birks, John Wiley, London (1975) p. 159. b) Y. Taniguchi, Y. Nishina, and N. Mataga, *Bull. Chem. Soc. Jpn.*, **43**, 764 (1972). c) J. Schroeder and F. Wilkinson *J. Chem. Soc., Faraday Trans. 2*, **75**, 896 (1979).
- 20) N. L. Weinberg and H. R. Weinberg, *Chem. Rev.*, **68**, 449 (1968). The value of 1.29 V vs. Ag | 0.1 N Ag<sup>+</sup> electrode listed in the reference must be corrected by +0.3 V for comparison with the other value vs. SCE.
- 21) M. E. Peover, *J. Chem. Soc.*, **1962**, 4540.
- 22) Y. Hirata, Y. Kanda, and N. Mataga, *J. Phys. Chem.*, **87**, 1659 (1983).
- 23) J. D. Simon and K. S. Peters, *J. Am. Chem. Soc.*, **105**, 4875 (1983).
- 24) K. Schested, H. Corfitzen, H. C. Christensen, and E. J. Hart, *J. Phys. Chem.*, **79**, 310 (1975).
- 25) H. P. Trommosdorf, P. Sahy, and J. Kahane-Pailous, *Spectrochim. Acta, Part A*, **26**, 1135 (1970).
- 26) B. T. Lim, S. Okajima, A. K. Chandra, and E. C. Lim, *Chem. Phys. Lett.*, **79**, 22 (1981).
- 27) a) H. Ootani, T. Kobayashi, K. Suzuki, and S. Nagakura, *Symposium on Molecular Structure*, Fukuoka, October 1980, Abstr. No. 4D23; b) N. Mataga, A. Karen, T. Okada, S. Nishitani, N. Kurata, Y. Sakata, and S. Misumi, *J. Am. Chem. Soc.*, **106**, 2442 (1984); c) H. Shioyama and N. Mataga, to be published.
- 28) An  $\epsilon_{IP}$  value may be approximated by the molar absorption coefficient of CA<sup>-</sup> ( $\epsilon_{CA^-}$ ). The  $\epsilon_{CA^-}$  values reported previously are: a)  $9.7 \times 10^3 \text{ dm}^3 \text{ mol}^{-1} \text{ cm}^{-1}$  in acetonitrile at 448 nm,<sup>10</sup> b)  $9.0 \times 10^3 \text{ dm}^3 \text{ mol}^{-1} \text{ cm}^{-1}$  in acetone at 450 nm (Y. Iida, *Bull. Chem. Soc. Jpn.*, **43**, 2772 (1970)), and c)  $7.7 \times 10^3 \text{ dm}^3 \text{ mol}^{-1} \text{ cm}^{-1}$  in ethanol at 454.5 nm (N. Sakai, I. Shirogami, and S. Minomura, *Bull. Chem. Soc. Jpn.*, **44**, 675 (1971)). The  $\epsilon_{CA^-}$  values fairly depend on solvent properties such as protic or aprotic solvent or solvent polarity. As the  $\epsilon_{IP}$  value, we here employed the  $\epsilon_{CA^-}$  value in acetone which is aprotic solvent with a dielectric constant (21.5) rather close to that of aprotic DCE (10.7).
- 29) This value which was estimated again by the same method as used in Ref. 4a is in good agreement with the previously reported value:  $(7.2 \pm 1.3) \times 10^3 \text{ dm}^3 \text{ mol}^{-1} \text{ cm}^{-1}$ .<sup>4a</sup>
- 30) This  $\epsilon_{CAH\cdot}$  value in DCE was determined by comparison with the known value:  $7.7 \times 10^3 \text{ dm}^3 \text{ mol}^{-1} \text{ cm}^{-1}$  (S. K. Wong, L. Fabes, W. J. Green, and J. K. S. Wan, *J. Chem. Soc. Faraday Trans. 1*, **68**, 211 (1972)) in 1,4-dioxane at 435 nm as a reference, assuming that the integrated intensity of CAH<sup>•</sup> absorption around 435 nm is independent on solvent.



31) Since the spectrum of  $\text{CA}^\cdot$  in  $\text{CH}_3\text{CN}$  was used as a reference of free  $\text{CA}^\cdot$  in the spectrum decomposition (Fig. 7), the value of  $\epsilon_{\text{CA}^\cdot}$  in  $\text{CH}_3\text{CN}$  might be also employed. However, the use of it did not alter the results in Table 1.

32) For example, the energy separations ( $E_R$ ) between the ground  $\text{CA}+\text{DH}$  and radical pair states in the  $\text{CA}-\text{DH}$  and  $\text{BP}-\text{DMA}$  systems are estimated nearly equal, because the H-atom transfer sites of both systems,  $>\text{C}=\text{O}$  and  $-\text{CH}_3$ , are very similar to each other. If the entropy changes for proton transfer in contact ion-pair (CIP) states,  $(\text{CA}^\cdot\cdots\text{DH}^+)_s$  and  $(\text{BP}^\cdot\cdots\text{DMA}^+)_s$ , leading to the formation of neutral radicals are approximately equal, the free energy change ( $\Delta G$ ) accompanying this reaction depends on the energy of CIP above the ground state ( $E_{\text{CIP}}$ ). The  $E_{\text{CIP}}$  values for  $(\text{CA}^\cdot\cdots\text{DH}^+)_s$  in DCE and  $(\text{BP}^\cdot\cdots\text{DMA}^+)_s$  in  $\text{CH}_3\text{CN}$  are estimated to be 134 and 305  $\text{kJ mol}^{-1}$ , respectively, and hence  $\Delta G$  value is larger for the  $\text{CA}-\text{DH}$  system than for the  $\text{BP}-\text{DMA}$  system. It has been measured that the energy of radical pair state produced in  $\text{BP}$ -aniline system in ethanol is 188  $\text{kJ mol}^{-1}$

above the ground state (L. J. Rothberg, J. D. Simon, M. Bernstein, and K. S. Peters, *J. Am. Chem. Soc.*, **105**, 3464 (1983)). Assuming that this value is approximately equal to the  $E_R$  value since the bond energies of C-H and N-H are also approximately equal to each other, the proton transfer from CIP is endothermic for the  $\text{CA}-\text{DH}$  system and exothermic for the  $\text{BP}-\text{DMA}$  system. The marked difference in  $k_p$  values for the two systems may be attributed to these conditions.

33) P. P. Levin, T. A. Kokrashvili, and V. A. Kuzmin, *Bull. Acad. Sci. USSR, Div. Chem. Sci.*, **31**, 466 (1982).

34) S. Yamamoto, K. Kikuchi, and H. Kokubun, *J. Photochem.*, **7**, 177 (1977).

35) M. M. Martin, N. Ikeda, T. Okada, and N. Mataga, *J. Phys. Chem.*, **86**, 4148 (1982).

36) N. Mataga and M. Ottolenghi, "Molecular Association," Vol. 2, ed by R. Foster, Academic Press, London (1979) p. 1.

---